Journal of Materials Chemistry C

Accepted Manuscript

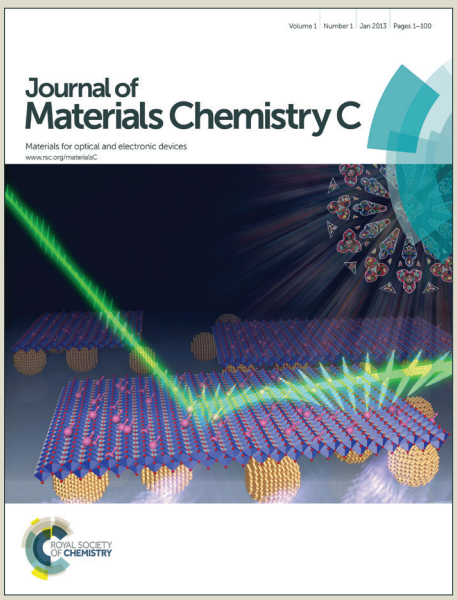

ROYAL SOCIETY OF CHEMISTRY

www.rsc.org/materialsC

Journal of Materials Chemistry C

RSCPublishing

ARTICLE

One step synthesis of fluorescent Carbon Dots through pyrolysis of N-hydroxysuccinimide

Cite this: DOI: 10.1039/x0xx00000x

C.S. Stan,[a] C. Albu,[a] A. Coroaba,[b] M. Popa[a] and D. Sutiman[a]

Received 00th January 2012,
Accepted 00th January 2012

DOI: 10.1039/x0xx00000x

www.rsc.org/

Abstract. Fluorescent Carbon Dots were prepared through a simple, straightforward, one step pyrolytic processing of N-Hydroxysuccinimide. The prepared C-Dots present remarkable photoluminescence with blue to green shifting emission and absolute quantum yields varying from 14 to 31% as a function of the excitation wavelength and selected dispersion mediums. Interestingly, upconversion from NIR to visible range was instrumentally recorded, the process being even visually observable. Further, the composition and morphology of the prepared C-Dots were studied using XPS, FT-IR, Raman, P-XRD, DLS and AFM investigation methods. Since the majority of C-Dots studies are biased towards fluorescent labeling in cellular imaging, their photoluminescence properties, physicochemical stability and ease of fabrication are expected to play a key role in applications ranging from sensors to efficient solar energy conversion or high performance optoelectronic devices.

Introduction

Carbon Dots are a new class of carbon based nanostructured materials which start to gather much research interest due to their remarkable properties such as tunable photoluminescence (PL) with high quantum yields (PLQY), lack of toxicity, chemical inertness, resistance to photobleaching [1]. Although their photoluminescence is counted as one of the most interesting features considering the wide applications potential, the exact PL mechanism is still an open debate subject. In a number of studies [2,3] the quantum confinement effect is considered to be responsible for C-Dots PL properties in a similar behavior with the "classic" semiconductor Quantum Dots while other opinions tend to emphasize the role of surface functional groups in achieving the excited states responsible for the excitation wavelength - dependent photo emission [4,5]. The search for an accurate description of the PL mechanism is further complicated by a significant number of studies which report up-conversion luminescence [6,7], usually from NIR (800-850 nm) to the blue-green area of the visible spectrum. Whilst the observed up-conversion PL of the C-Dots is still controversial [8], this feature, if confirmed, may be highly regarded for the bio-imaging applications [9] or by the attempts of further increasing the efficiency of solar energy conversion systems [10].

As a consequence of the significant interest for the C-Dots, an increasing number of preparation paths were reported, generally divided into two main categories: chemical and physical methods. The chemical methods include electrochemical [11], thermal [12], combustion [13], acidic oxidation [14] with certain variations where the main process is microwave or ultrasonic assisted [15,16]. Physical methods including arc discharge [17], laser ablation [18] or plasma treatment [19] are using various carbon sources like carbon nanotubes graphite or graphite oxide, the obtained C-Dots usually requiring further surface treatment or passivation in order to increase the hydrophilicity and PL emission.

In most cases the chemical methods are significantly less demanding in terms of required equipment or starting materials used as carbon sources having the additional advantage of producing already surface functionalized C-Dots. Several reported preparation paths leading to highly fluorescent, tunable emission C-Dots used various commonly available materials or compounds as carbon source. Among the most interesting or unusual approaches plant soot [20], L-glutamic acid [21], ethanolamine [22], glucose [23], even orange or banana juice and soluble coffee [24-26] were thermally processed to obtain fluorescent C-Dots.

In the present study, a facile one step pyrolysis processing of N-Hydroxysuccinimide (NHS) is described. Preliminary experimental parameters (temperature range, duration) of the pyrolytic decomposition of NHS were established through thermogravimetric analysis. The choice for NHS is based on our preliminary experiments which revealed its suitability for producing high quality C-Dots in terms of PL properties, most probable due to some particular physical-chemical properties such as: relatively low melting point (~98 °C), favorable decomposition scheme, presence of the succinic ring and various functional groups (carbonyl, imide) which have an important role in achieving the targeted properties [27]. Also NHS is a commonly available, low cost compound with many uses in organic synthesis and pharmaceutics.

The resulted C-Dots are strongly photoluminescent in a relatively wide excitation range (350-420 nm) and easily dispersible in various solvents including water, ethylic alcohol, or acetone. Besides the previously reported PL emission dependence on the excitation wavelength, the variation of the PL properties according to the dispersion medium and up-conversion from NIR to visible spectrum were also noted and experimentally confirmed.

Experimental

Materials

N-Hydroxysuccinimide (97%) was purchased from Sigma-Aldrich. Milli-Q water was used during preparation, purification and dimensional selection procedures. Reagent grade ethanol (EtOH) and acetone from Merck Chemicals were used as re-dispersion mediums.

Preparation

In a typical synthesis procedure, 3g of NHS is added in a 50 mL three neck Schlenk flask provided with a magnetic stirrer and a temperature controlled heating mantle. The temperature is raised to the melting point of NHS (~ 98 ^{o}C) when the magnetic stirring is started. From this stage, the reaction undergoes in N_2 atmosphere, the temperature being gradually raised (about 10^{o}C/min.) to 180 ^{o}C and maintained at this value for 30 min. Then, the entire content of the flask is quickly transferred in 40 mL cold water and allowed to reach the room temperature. The mixture is centrifuged at 5000 RPM for about 30 min. The resulted deep brown tinted supernatant is collected and additionally centrifuged at 15000 RPM for 10 min. Again, the resulted brownish tinted aqueous supernatant containing dimensionally selected C-Dots is collected and further freeze dried. The prepared C-Dots dried or re-dispersed in water, EtOH and acetone are kept as such for investigation purposes.

Methods

XPS analysis was performed on a KRATOS Axis Nova, using AlKα radiation, with 20 mA current, 15 kV voltage. The incident X-ray beam was focused on a 0.7 mm x 0.3 mm area of the surface. The wide XPS spectra was collected in the range of -10÷1200 eV with a resolution of 1 eV and a pass energy of 160 eV. The high resolution spectra for all the elements identified from the survey spectra were collected using a pass energy of 20 eV and a step size of 0.1 eV. The FT-IR spectra were recorded in the 400 - 4000 cm-1 range, using a Bruker Vector 22 spectrometer, according to KBr pellet method. The Raman spectroscopy was performed in the 100 - 3200 cm^{-1} range with a Renishaw inVia Reflex confocal microscope equipped with a He-Ne laser at 633 nm (17 mW) and a CCD detector coupled to a Leica DM 2500M microscope. All measurements were made in backscattering geometry using a 50x objective with a numerical aperture (NA) value of 0.75. The XRD patterns were recorded in the 5 - 85º 2 Theta range, on a Panalytical X'Pert Pro diffractometer provided with a Cu-Kα radiation source (λ = 0,154060 nm). Dimensional analysis (DLS) was performed on Shimadzu SALD-7001 equipment. Prior to investigation the aqueous C-Dots dispersion was sonicated for about 10 min. The steady state fluorescence, chromaticity and absolute quantum yields (PLQY) were recorded on a Horiba Fluoromax 4P provided with the Quanta-φ integration sphere. The AFM measurements were performed using a Ntegra Spectra – NT-MDT, Russia instrument operated in tapping mode under ambient conditions. Silicon cantilever tips (NSG 10) with a resonance frequency of 140-390 kHz, a force constant of 5.5-22.5 Nm^{-1} and 10 nm tip curvature radius, were used. The sample was prepared by spin-coating at 1300 RPM the acetone dispersed C-Dots on a glass slide by means of a Laurell WS-400-6NPP Spin Coater. TEM investigations were performed by means of Hitachi HT-7700 equipment, operated at 100 kV accelerating voltage, in high contrast mode. The C-Dots samples were deposited from a highly diluted solution on 300 mesh carbon plated, copper grids.

Visual testing of photo-luminescent properties was performed using a Philips UVA TL4WBLB lamp with the emission maximum located in the 370-390 nm range and a 50mW, 440nm laser diode.

Results and Discussion

Figure 1(a) summarizes the process taking place during pyrolysis of NHS leading to C-Dots. Related experiments performed at higher temperatures (200-240 °C) or longer thermal processing (45-90 min) time yielded significantly lower PL emission C-Dots due to advanced thermal destruction. In the optimized process (180 °C, 30 min), remnant quantities of NHS may act as a passivation agent which along with various functional groups located on the surface of the C-Dots provide the conditions for reaching intense PL and high PLQY. This conclusion is sustained by the thermal analysis of NHS (supporting information, Figure S1) which revealed important mass losses (over 50%) in 200- 250 °C interval through volatiles exhausting, as a result of advanced destructuration, which drastically depletes the amount of the functional groups located on the surface. Figure 1(b,c) presents the visually tested emission of the prepared C-Dots dispersed in water under excitation with a UVA laboratory lamp (b) and a 440 nm laser (c). As could be noted, the excitation-dependent emission is clearly highlighted, the PL emission being shifted from blue to green. Chromaticity parameters according to CIE 1931 color space recorded at 360 nm and 420 nm excitation wavelengths are included in supporting information, Figure S3.

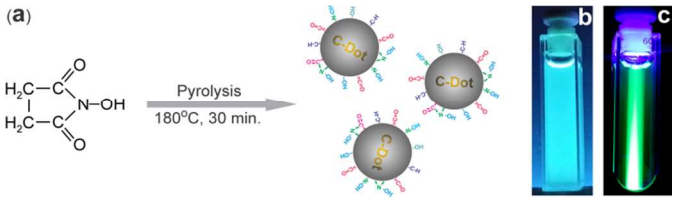

Figure 1. (a) NHS pyrolysis scheme leading to C-Dots, (b) water dispersed C-Dots under UVA excitation and (c) under 440 nm laser excitation

XPS investigation revealed the relative concentrations of various functional groups (Figure 2 a-c). The high resolution C 1s spectrum clearly highlighted the graphitic core by the sp^2 bonded carbons (Figure 2.a) along with the existence in high concentrations of carbonyl groups which, as presented later, could be responsible for the radiative transitions involved in the fluorescent emission of the C-Dots.

The relatively high (15%) single bonded carbons is in agreement with the Raman investigation which also indicates the structural defects of the graphitic core, most probably due various edge or surface located functional groups. The surface rich functional groups is highlighted also by the high resolution O 1s and N 1s spectra, being in close agreement with the recorded FT-IR analysis. The overall O, N, C concentrations as resulted from the XPS survey spectrum is presented in Table 1.

Table 1. Overall C, N, O concentrations recorded for the prepared C-Dots

Element	O	N	C
Atomic concentration (%)	26.44	14.12	59.44
Mass concentration (%)	31.70	14.82	53.48

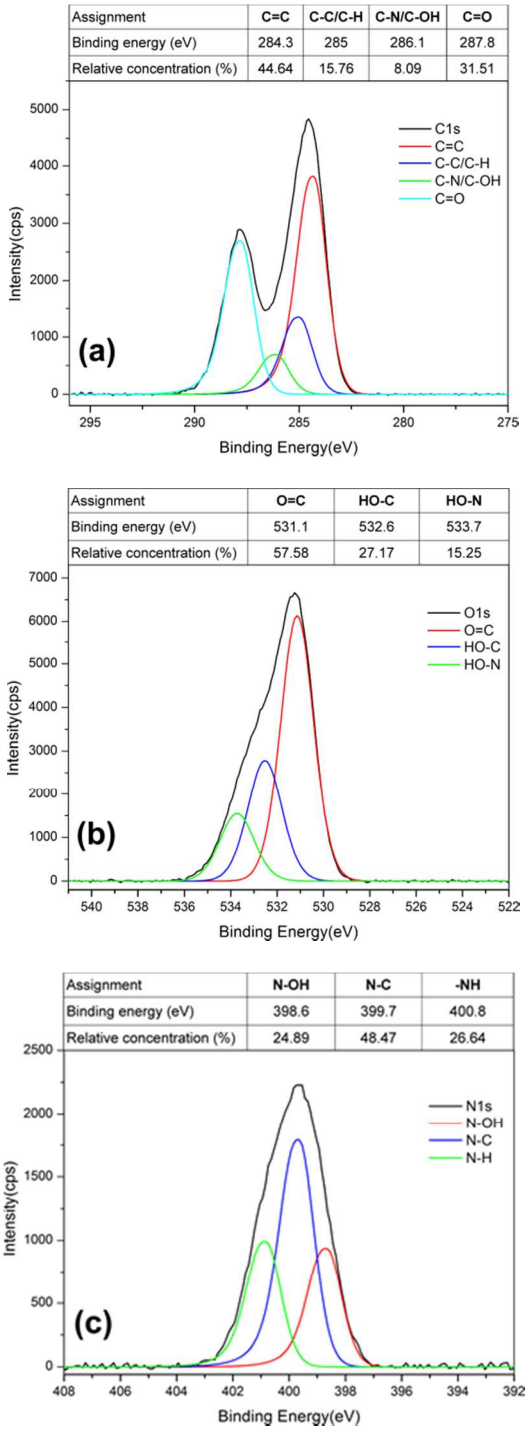

Figure 2. High resolution XPS spectra of (a) C 1s, (b)O 1s, (c) N 1s and relative concentrations of various functional groups

Figure 3 shows the recorded Raman spectrum of the prepared C-Dots. The peaks centered at 1365 and 1565 cm^{-1} are typical signatures for graphitic nanostructures, being in close accordance with other works [15,21]. The slight displacements of these peaks in various reported works is due to the laser parameters used for the Raman excitation in a specific measurement setup [28]. The 1565 cm^{-1} peak (G band) correspond to the in-plane stretching vibration E_{2g} mode of graphite, being related to sp^2 bonded carbon atoms while the 1365 cm^{-1} (D band) originates from the swinging bonds vibrations of carbon atoms located in the edge plane of disordered graphite, being often referred as the disorder or defect band. The intensity ratio between the D and G bands (I_D/I_G) is proportional with the disorder degree/presence of the structural defects and also indicates the ratio of sp^3/sp^2 carbon [1,29]. The prepared C-Dots present an over-unity I_D/I_G ratio suggesting the intercalation of nitrogen atoms in the carbonaceous core and/or the presence of surface located edge functional groups leading to a somehow disordered structure. The assumed functional groups rich structure of the prepared C-Dots is consistent with the results provided by FT-IR analysis (Figure 4).

A multitude of peaks related to various functional groups are present in the recorded IR spectrum (see imprinted table in Figure 4).

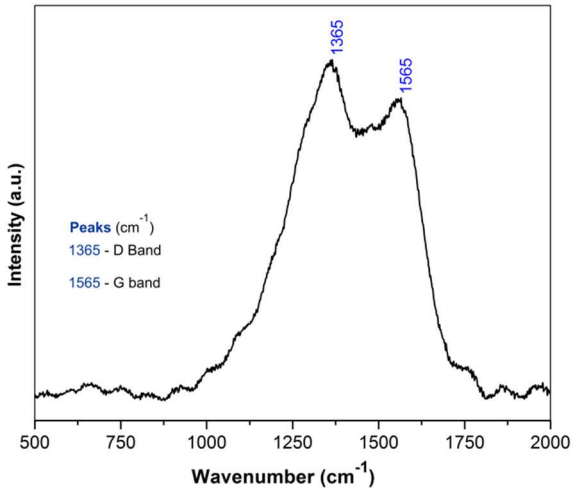

Figure 3. Recorded Raman spectrum

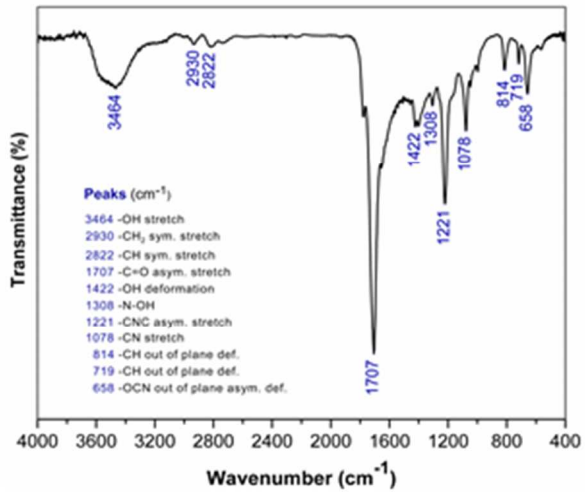

Figure 4. Recorded FT-IR spectrum including functional groups assignment

In fact, the recorded spectrum of the prepared C-Dots is quite similar with the one recorded for NHS (supporting information, Figure S2). Although most of the peaks are still present, in certain cases slightly displaced due to the structural

rearrangements, the significant difference relies on the ratio between the recorded peaks. While in the unprocessed NHS the ratio between -CNC- asym. stretch (1220 cm^{-1}) and –C=O asym. stretch (1707 cm^{-1}) is almost 2/3, in case of prepared C-Dots the value drops under ½ due to the losses occurring during the thermal processing. Same situation is also noticeable in case of other peaks corresponding to various functional groups. The presence of various functional groups, especially carbonyls and nitrogen containing groups, located on the surface of the C-Dot is fundamentally important for their PL properties [4,30].

As lately described, the interaction of surface located functional groups with the dispersing solvents significantly alters the PL properties, especially the PLQY. As stated above, the pyrolysis parameters are particularly important in obtaining highly luminescent C-Dots, an advanced thermal destruction accompanied by nitrogen rich volatiles exhaustion is leading to poorer functional groups containing.

Figure 5 shows the XRD pattern recorded for the investigated C-Dots. The relatively broad peak located at 27.48° 2θ is slightly upward shifted compared to the classic graphite peak located at 26.4° 2θ, corresponding to a minor decrease of the spacing between carbon layers from 0.337 nm to 0.324 nm in case of C-Dots. The slightly reduced spacing between the carbon layers could be explained by interactions occurring between terminal functional groups, for example by the hydrogen bonding between -OH groups.

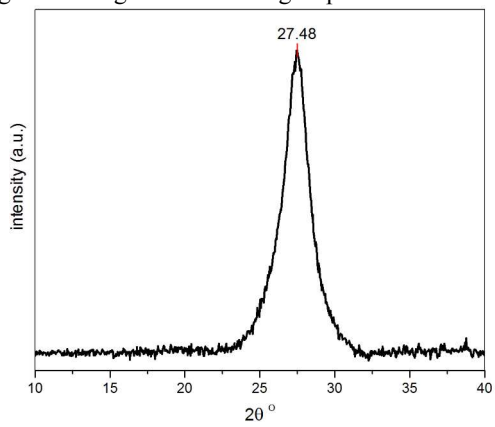

Figure 5. XRD pattern of the prepared C-Dots

The preparation of samples for AFM investigation proved to be difficult due to the encountered agglomeration tendency even when a high dilution acetone C-Dots solution was drop spread on the glass surface. The agglomeration tendency was also previously reported in other works [31] and solved by spin coating of the highly diluted solution on several glass slides subjected to investigation. Even so, AFM images revealed the existence of both small particles in the range of 20-50 nm as well as elongated aggregates (Figure 6a, c), most probable due to the rapid drying and preferred orientation occurring during spin coating. The results are in good agreement with the DLS analysis which revealed a 20-30 nm average size of the prepared C-Dots dispersed in water (Figure 6b). TEM investigations were performed on the samples prepared by drop spreading high diluted C-dots in EtOH on carbon coated, 300 mesh copper grids.

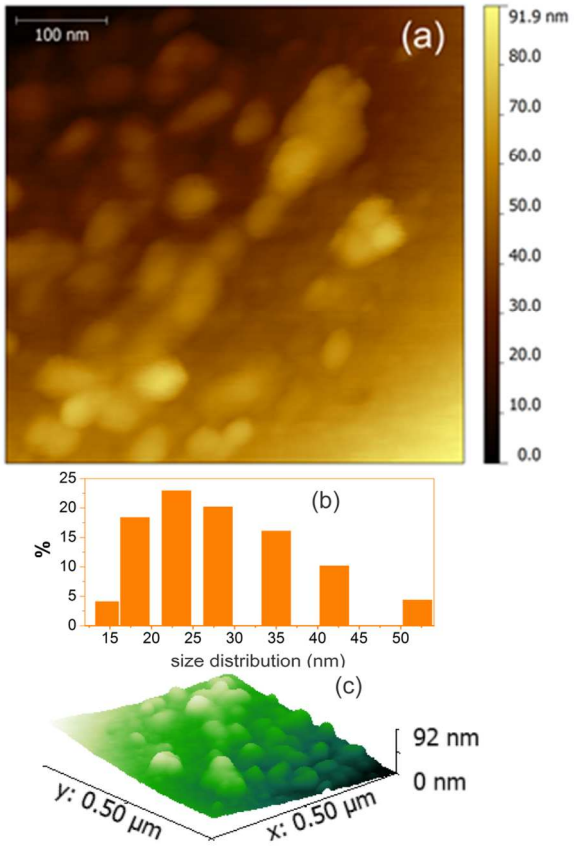

Figure 6. (a) Recorded AFM image, (b) DLS recorded size distribution, (c) 3D AFM image of prepared C-Dots

Fig. 7(a) reveals aggregates in 50 – 200 nm range due to the already mentioned particle-agglomeration tendency, which is also highlighted by AFM investigation. A significant insight on the fine structuring of the aggregates is visible in the micrograph recorded at higher magnification, Fig. 7(b). As may be also noted in Fig. 7(b), both aggregates (arrows 1 and 2) have granular appearance with finer visible details, which highlight the presence of differentiated entities suggesting the presence of very small C-Dots in 2-5 nm range in relation to the dimension of aggregates (1: approx. 120 nm; 2: approx. 20 nm).

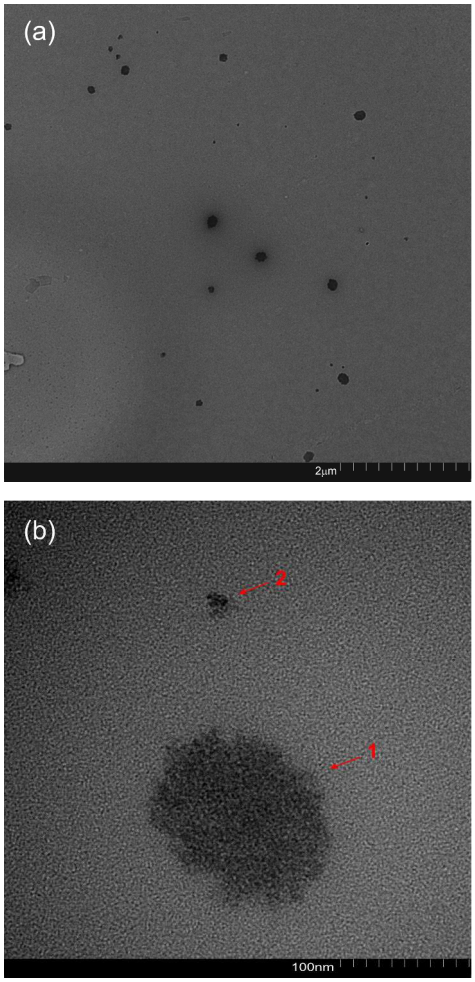

Figure 7. TEM images recorded at (a) 35k and (b) 700k magnifications

Fluorescence spectroscopy investigation

For the fluorescence related investigations, three samples were prepared by dispersing in each of them 1mg freeze dried C-Dots in 3 mL H_2O, EtOH and acetone respectively. The steady state fluorescence spectra (Figure 8a-c) were recorded in 350-420 nm (10 nm step) excitation range whereas the up-converted emission (Figure 8d) was studied in the 750-960 nm excitation range. As could be noted, the shifting of the down-conversion PL emission peaks according to the excitation wavelength occurs in all three cases. The Stokes shift and the recorded intensities are also significantly solvent dependent. In case of water dispersed C-Dots the emission peaks are located in 437-516 nm range (Figure 8a) with larger Stokes shifts while in case of acetone dispersed C-Dots (Figure 8c) the range is significantly narrower (447-493 nm), the Stokes shifts being accordingly lower. In case of Et-OH dispersed C-Dots (Figure 8b) an in between situation was encountered (442-505 nm). The emission intensities were noticeable lower for water dispersed C-Dots compared with EtOH and acetone dispersed C-Dots. The recorded results from steady state fluorescence are in agreement with the absolute PLQY measurements, where the highest QY (31.74%) was recorded for acetone dispersed C-Dots. Table 2 presents the absolute PLQY values recorded at different excitation wavelengths.

Table 2. Absolute PLQY of the C-Dots dispersed in H_2O. EtOH and acetone

Sample/ solvent	**absolute PLQY** (%)					
	excitation wavelength (nm)					
	370	*380*	*390*	*400*	*410*	*420*
C-Dots /H_2O	14.22	16.45	18.60	20.57	22.93	23.62
C-Dots /EtOH	14.23	16.86	19.08	21.53	24.38	24.96
C-Dots /acetone	17.59	21.07	23.77	25.37	30.59	31.74

The results clearly indicate interactions between the solvent and surface located functional groups. Thus, as the polarity of the solvent increases (acetone → EtOH → H_2O) the PL intensity and PLQY decreases. The peak emission range is also shifted to higher wavelengths as the polarity of the solvent increases, lower energy photons being produced in the radiative processes. This indicates an excitation energy loss through various non-radiative deactivation processes. A possible explanation of the lower PL and PLQY recorded for water dispersed C-Dots is a less efficient transfer of the excitation radiation to the states responsible for the PL emission due to the vicinity of the –OH oscillators which are known to strongly quench the PL emission through vibronic coupling deactivation paths. In the most favorable case of acetone dispersed C-Dots the surface located functional groups responsible for the PL emission are significantly less disturbed while the non-radiative deactivation paths being no more present. Luminescence properties of C-Dots are rather a result of the radiative transitions occurring within or between the functional groups located on the C-Dots surface and seem to be less dependent on their size. Recent studies emphasize the role of functional groups such as carbonyl, carboxyl and nitrogen containing groups in PL properties of C-Dots and the possibility to alter the PL emission through modification of these surface localized groups. The surface located functional groups may be responsible for various trapping states, each with different energy level, leading to an excitation dependent emission [4,32,33]. The dimensional characteristics of C-Dots may be important to a certain extent in achieving the PL properties but we suspect an indirect relation between them. In various works related to C-Dots, similar PL properties were reported in case of <10 nm C-Dots [20,21] but, also for those in the 10-50 nm range [24,31,34]. One possible assumption is that a noticeable PL is achieved between certain dimensional limits. Beyond the upper limit, an oversized carbonaceous core may be less decorated with surface localized functional groups or these groups are less packed to achieve the type of interactions responsible for triggering the PL emission. The PL mechanism relying on functional groups attached on the surface of the C-Dots may provide an additionally insight on observed excitation wavelength dependence of the emission peaks. While in certain studies [2,3] this dependence is explained by the concomitant presence of various dimensional species, each of them

responsible by a particular emission peak, the functional group based PL can explain it by the excited states achieved within or between various functional groups, each responsible for a particular emission peak.

The recorded up-conversion PL is not excitation wavelength dependent (Figure 8d) but, the PL emission peaks are different in each solvent medium (471 nm in acetone, 489 nm in EtOH and 502 nm in H_2O). In all cases the excitation peaks are recorded at 838-840 nm. Also, as in case of down-conversion fluorescence, the PL intensity is influenced in the same way by the polarity of the solvent. Lower PL intensity and anti-Stokes shift (~340 nm) were recorded for water dispersed C-Dots while the most favorable situation was met again in case of acetone dispersed C-Dots (~370 nm).

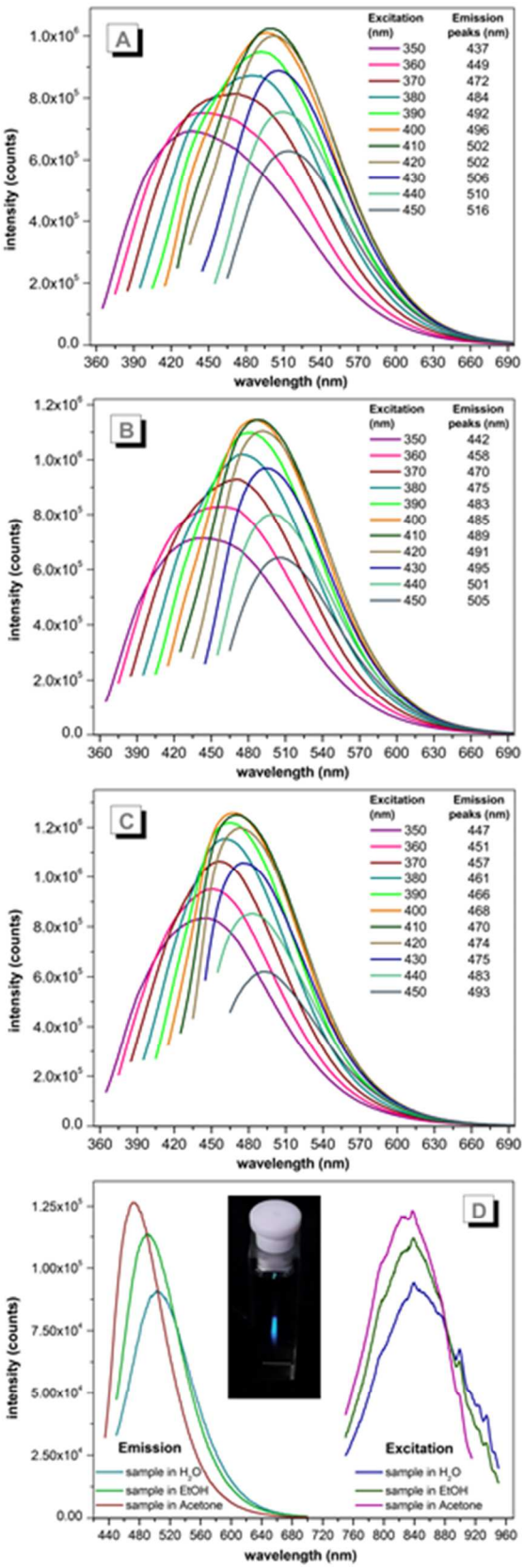

Figure 8. PL emission recorded for excitation wavelengths from 350 to 450 nm in 10 nm increments of the prepared C-Dots dispersed in (a) water, (b) EtOH, (c) acetone and (d) up-conversion emission recorded for the same samples

Although the up-conversion mechanism in C-Dots is not entirely understood, a multi-photonic process is generally accepted [1,6,7] till further clarifications. The up-converted PL emission is easily noticed with the naked eye as could be observed in the Figure 8d embedded picture.

Conclusions

Highly fluorescent Carbon Dots were prepared through one step pyrolytic processing of N-Hydroxysuccinimide using a non-demanding experimental setup. The PL emission and absolute PLQY were studied in detail in several dispersion mediums. Besides the previously reported shifting of the emission peaks according to the excitation wavelength, the intensities, Stokes shifts and absolute PLQY were found to be markedly dependent on the polarity of the dispersing solvent. Based on the recorded results, we suggest that fluorescent properties of C-Dots are rather a result of the radiative processes occurring within or between the functional groups located on the C-Dots surface and less dependent on their size. Up-conversion from NIR (840 nm) to VIS (479-502 nm) were instrumentally confirmed, the process being also visually noticeable. In depth investigation of the prepared C-Dots through XPS, Raman, FT-IR, P-XRD investigations revealed the graphitic nature of the prepared C-Dots and also the abundance of various surface located functional groups. DLS and AFM were used to study the morphology of the prepared C-Dots.
Although the majority of C-Dots related studies are focused on bio-imaging, their luminescent properties and ease of fabrication are expected to play a key role in applications ranging from sensors to efficient solar energy conversion or high performance optoelectronic devices.

Acknowledgements

This work was supported by a grant of the Romanian National Authority for Scientific Research, CNCS – UEFISCDI, project number PN-II-ID-PCE 2011-3-0708 - PN-II IDEI 335/2011.

Notes and references

[a] TUIasi - Gheorghe Asachi Technical University of Iasi, Faculty of Chemical Engineering and Environmental Protection, 73 Prof. Dr. docent Dimitrie Mangeron, 700050, Iasi, Romania. Fax: 0040 232 271311; Tel: 40 - 232 278683; E-mail: stancs@tuiasi.ro.

[b] Petru Poni Institute of Macromolecular Chemistry, 41A Aleea Grigore Ghica Voda, Iasi, Romania.

† Electronic Supplementary Information (ESI) available: [details of any supplementary information available should be included here]. See DOI: 10.1039/b000000x/

1 H. Li , Z. Kang, Y. Liu, S.T. Lee, *J. Mater. Chem.*, 2012, **22**, 24230-242353.
2 H. Li, X. He, Z. Kang, H. Huang, Y. Liu, J. Liu, S. Lian, C.H.A. Tsang, X. Yang, S.T. Lee, *Angewande Chem.*, 2010, **49**, 4430-4434.
3 Y. Xu, M. Wu, Y. Liu, X.Z. Feng, X.B. Yin, X.W. He, Y.K. Zhang, *Chemistry – A European Journal*, 2013, **19**, 2276–2283.
4 Y. Deng, X. Chen, F. Wang, X. Zhang, D. Zhao, D. Shen, *Nanoscale*, 2014, **17**, 10388-10393.
5 D. Tan, S. Zhou, Y. Shimotsuma, K. Miura, J. Qiu, *Optical Materials Express*, 2014, **4**, 213-219.
6 S. Gomez de Pedro, A. Salinas-Castillo, M. Ariza-Avidad, A. Lapresta-Fernández, C. Sánchez-González, C.S. Martínez-Cisneros, M. Puyol, L.F. Capitan-Vallvey, J. Alonso-Chamarro, *Nanoscale*, 2014, **6**, 6018-6024.
7 Salinas-Castillo A, Ariza-Avidad M, Pritz C, Camprubí-Robles M, Fernández B, Ruedas-Rama MJ, Megia-Fernández A, Lapresta-Fernández A, Santoyo-Gonzalez F, Schrott-Fischer A, *Chem. Commun.*, 2013, **49**, 1103-1105.
8 X. Wen, P. Yu, Y.R. Toh, X. Ma, J. Tang, *Chem. Commun.*, 2014; **50**, 4703-4706.
9 Y. Song, S. Zhua, B. Yang, *RSC Adv.*, 2014, **4**, 27184-27200.
10 C. Wang, X. Wu, X. Li, W. Wang, L. Wang, M. Gu, Q. Li, *J. Mater. Chem.*, 2012, **22**, 15522-15525.
11 H. Ming, Z. Ma, Y. Liu, K. Pan, H. Yu, F. Wang, Z. Kang, *Dalton Trans.*, 2012, **41**, 9526-9531.
12 X.W. Tan, A.N.B. Romainor, S.F. Chin, S.M. Ng, *J. Anal. Appl. Pyrol.*, 2014, **105**, 157–165.
13 K.M. Tripathi, A.K. Sonker, S.K. Sonkar, S. Sarkar, *RSC Adv.*, 2014; **4**, 30100-30107.
14 K. Wang, Z. Gao, G. Gao, Y. Wo, Y. Wang, G. Shen, D. Cui, *Nanoscale Res. Lett.*, 2013, **8**, 122-131.
15 X. Zhai, P. Zhang, C. Liu, T. Bai, W. Li, L. Dai, W. Liu, *Chem. Commun.*, 2012, **48**, 7955–7957.
16 L. Hui, Y.X. Xi, Z.J. Jia, L.Y. Fang, H.C. Zhi, *Scientia Sinica Chimica*, 2013, **43**, 895-900.
17 X. Xu, R. Ray, Y. Gu, H.J. Ploehn, L. Gearheart, K. Raker, W.A. Scrivens, *J. Am. Chem. Soc.*, 2004, **126**, 12736-12737.
18 V. Thongpool, P. Asanithi, P. Limsuwan, *Procedia Eng.*, 2012, **32**, 1054–1060.
19 T. Gokus, R.R. Nair, A. Bonetti, M. Böhmler, A. Lombardo, K.S. Novoselov, A.K. Geim, A.C. Ferrari, A. Hartschuh, *ACS Nano*, 2009, **3**, 3963–3968.
20 M. Tan, L. Zhang, R. Tang, X. Song, Y. Li, H. Wu, Y. Wang, G. Lv, W. Liu, X. Ma, *Talanta*, 2013, **115**, 950–956.
21 X. Wu, F. Tian, W. Wang, J. Chen, M. Wub, J.X. Zhao, *J. Mater. Chem.*, 2013, **1**, 4676-4684.
22 X. Dong, Y. Su, H. Geng, Z. Li, C. Yang, X. Li, Y. Zhang, *J. Mater. Chem.*, C, 2014, **2**, 7477-7481. doi: 10.1039/C4TC01139B
23 Z. Ma, H. Ming, H. Huang, Y. Liu, Z. Kang, *New J. Chem.*, 2012, **36**, 861-864.
24 S. Sahu, B. Behera, T.K. Maiti, S. Mohapatra, *Chem. Commun.*, 2012, **48**, 8835-8837.
25 B. De, N. Karak, *RSC Adv.*, 2013, **3**, 8286–8290.
26 C. Jiang, H. Wu, X. Song, X. Ma, J. Wang, M. Tan, *Talanta*, 2014, **127**, 68–74.
27 P.C. Hsu, H.T. Chang, *Chem. Commun.*, 2012, **48**, 3984-3986.
28 K. Satoa, R. Saito, Y. Oyama, J. Jiang, L.G. Cançado, M.A. Pimenta, A. Jorio, G.G. Samsonidze, G. Dresselhaus, M.S. Dresselhaus, *Chem. Phys. Lett.*, 2006, **427**, 117–121.
29 A. Jorio, E.H. Martins Ferreira, M.V.O. Moutinho, F. Stavale, C.A. Achete, R.B. Capaz, *Physica Status Solidi (b)*, 2010, **247**, 2980–2982.
30 L.H. Mao, W.Q. Tang, Z.Y. Deng, S.S. Liu, C.F. Wang, S. Chen, *Ind. Eng. Chem. Res.*, 2014, **53**, 6417–6425.
31 S.C. Ray, A. Saha, N.R. Jana, R. Sarkar, *J. Phys. Chem. C.*, 2009, **113**, 18546–18551.

32 K. Hola, A.B. Bourlinos, O. Kozak, K. Berka, K.M. Siskova, M. Havrdova, J. Tucek, K. Safarova, M. Otyepka, E.P. Giannelis, *Carbon*, 2014, **70**, 279-286.
33 R. Tian, S. Hu, L. Wu, Q. Chang, J. Yang, J. Liu, *Appl. Surf. Sci.*, 2014, **301**, 156-160.
34 J. Shen, Y. Zhu, C. Chen, X. Yang, C. Li, *Chem. Commun.*, 2011, **47**, 2580–2582.

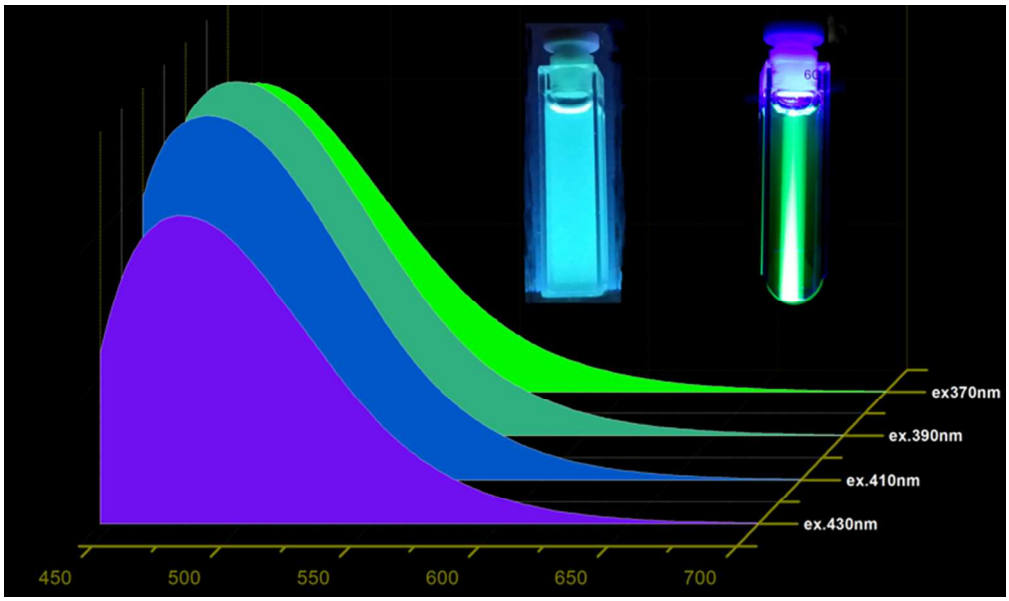

67x39mm (300 x 300 DPI)